

UNIVERSAL SHAPES AND BIFURCATION FOR ROTATING
INCOMPRESSIBLE FLUID DROPS

Donald R. Smith and James E. Ross

ABSTRACT. Axisymmetric shapes of Beer, Rosenthal, D. Ross, Gulliver, and others provide universal solutions for a problem related to Plateau's rotating drops, for the material class of Noll's simple incompressible fluid subject to Laplace's frequently used linear constitutive relation between pressure jump and mean curvature at the free boundary. A bifurcation from spheroidal to toroidal shapes occurs within this family, leading initially to a decrease in angular momentum. It is shown that the spheroidal and toroidal axisymmetric families connect tangentially in the angular speed-angular momentum plane, and the corresponding bifurcation slope is calculated. It is also shown for a general (possibly nonaxisymmetric) rigidly rotating drop without body force that the center of mass of the drop is necessarily on the axis of rotation, complementing a result of Wente.

1. Preliminary results

The steady rigid rotation of a homogeneous incompressible fluid drop which is surrounded by a rigidly rotating incompressible fluid is considered; see Ross and Smith [12] for a discussion of relevant experiments of Plateau [7], Wang, Trinh, Croonquist, and Elleman [16], and others. An interfacial surface separates the drop from the surrounding fluid, and interfacial surface tension balances the pressure gradients due to the rotational acceleration. The rotating drop occupies a domain $\mathcal{D}_1 = \mathcal{D}_1(t)$ at time t and the surrounding fluid occupies an outer domain $\mathcal{D}_2 = \mathcal{D}_2(t)$ enclosing \mathcal{D}_1 . The fluids are incompressible homogeneous simple fluids of respective mass densities ρ_1 and ρ_2 , and they undergo separate steady rigid rotations about a common axis with respective angular rotation speeds ω_1 and ω_2 . (A *simple fluid* is a simple material (in the sense of Noll) that has maximal symmetry, with symmetry group consisting of the entire unimodular group; cf. Smith [13].)

A steady rigid rotation about an axis takes initial points $X = (X_1, X_2, X_3)^T$ into points $x = (x_1, x_2, x_3)^T$ at time t with

$$x \equiv x(X, t) = F(t)X, \quad F(t) = \begin{pmatrix} \cos \omega t & \sin \omega t & 0 \\ -\sin \omega t & \cos \omega t & 0 \\ 0 & 0 & 1 \end{pmatrix}$$

where ω is the angular speed and Cartesian coordinates are used with the x_3 -axis taken to coincide with the axis of rotation, and the origin is placed on the axis of rotation. For brevity, the notations x and X are used for points and also for the corresponding vectors that translate the origin to the given points. A routine calculation based on the

Received June 21, 1993.

1991 *Mathematics Subject Classification*: 34A47.

Key words and phrases: bifurcation, surface tension, rotating fluid.

balance of linear momentum shows that any such steady rigid rotation with constant angular speed ω is dynamically possible for any homogeneous incompressible simple fluid of constant mass density ρ in the absence of body force, with resulting Cauchy stress $T(x) = -p(x)I$ with pressure $p(x) = \frac{1}{2}\rho\omega^2r^2 + p_0$ for a suitable constant p_0 and where r is distance from the axis of rotation (cf. Exercise 8.4.3 of Smith [13]). For the rotating drop and the surrounding rotating fluid, this result yields for the respective Cauchy stresses $T_1(x)$ and $T_2(x)$,

$$T_i(x) = -p_i(x)I \quad \text{with} \quad p_i(x) = \frac{1}{2}\rho_i\omega_i^2r^2 + p_0^{(i)}, \quad \text{for } i = 1, 2, \quad (1.1)$$

for suitable constants $p_0^{(1)}$ and $p_0^{(2)}$, where r denotes distance from the common axis of rotation.

The two rotating fluids are separated by an interfacial surface membrane modelled by the smooth boundary surface $\partial\mathcal{D}_1$ along with the following linear constitutive relation of Laplace between the membrane pressure jump and mean curvature

$$p_1(x) - p_2(x) = 2\sigma H(x) \quad (1.2)$$

for points x on the boundary surface $\partial\mathcal{D}_1$, where $H(x)$ is the mean curvature of the surface at x , and σ is a fixed positive constant which is the coefficient of interfacial surface tension. From (1.1) and (1.2) follows the free-boundary equation

$$2\sigma H(x) = p_0 + \frac{1}{2}(\rho_1\omega_1^2 - \rho_2\omega_2^2)r^2 \quad (1.3)$$

for points on the surface, with constant $p_0 := p_0^{(1)} - p_0^{(2)}$. Equation (1.3) can also be obtained as the Euler/Lagrange equation for a suitable variational problem; cf. Ross and Smith [12]. For brevity we often identify the drop and its domain, referring to the “drop \mathcal{D}_1 ”.

Theorem 1.1. *The free-boundary condition (1.3) implies that the center of mass of the rigidly rotating drop \mathcal{D}_1 is on the axis of rotation.*

Proof. In the case $\rho_1\omega_1^2 = \rho_2\omega_2^2$ it follows from a theorem of Alexandrov [1] that the sphere is the only compact embedded surface (enclosing a positive volume) satisfying (1.3), and so the stated result is true in this case. Hence we need only consider further the case $\rho_1\omega_1^2 \neq \rho_2\omega_2^2$. Multiply (1.3) by the exterior directed unit normal vector $\vec{n}(x)$ for points x on the boundary surface of \mathcal{D}_1 and integrate with respect to surface area over the surface of the drop to find

$$\begin{aligned} \int_{\partial\mathcal{D}_1} H(x)\vec{n}(x) dA(x) &= \frac{1}{2\sigma}p_0 \int_{\partial\mathcal{D}_1} \vec{n}(x) dA(x) \\ &\quad + \frac{1}{4\sigma}(\rho_1\omega_1^2 - \rho_2\omega_2^2) \int_{\partial\mathcal{D}_1} (x_1^2 + x_2^2)\vec{n}(x) dA(x). \end{aligned} \quad (1.4)$$

An integration by parts with the divergence theorem shows that the first integral on the right side vanishes

$$\int_{\partial\mathcal{D}_1} \vec{n}(x) dA(x) = 0. \quad (1.5)$$

The integral on the left side of (1.4) also vanishes

$$\int_{\partial\mathcal{D}_1} H(x)\vec{n}(x) dA(x) = 0 \quad (1.6)$$

as follows from the known fact that the integrand $H\vec{n}$ is proportional to the surface Laplacian of the position vector (cf. equation (17.33) of Laugwitz [6]), so that an integration by parts *in the surface* $\partial\mathcal{D}_1$ yields (1.6). From (1.4)–(1.6) with $\rho_1\omega_1^2 \neq \rho_2\omega_2^2$ follows $\int_{\partial\mathcal{D}_1} (x_1^2 + x_2^2)\vec{n}(x) dA(x) = 0$, and then integration by parts in this last result yields $\int_{\mathcal{D}_1} x_j dV(x) = 0$ (for $j = 1, 2$), from which the stated assertion follows. \square

A theorem of Wente [17] shows that the drop has a plane of symmetry perpendicular to the rotational x_3 -axis. We take the origin of coordinates to be placed on the rotational axis at the center of mass of the drop, and then Wente's theorem implies that the drop is symmetric across the x_1x_2 -plane $x_3 = 0$.

Any suitable drop region $\mathcal{D} = \mathcal{D}_1$ with boundary satisfying the free-boundary equation (1.3) corresponds to a universal solution for the stated mathematical problem in the class of simple incompressible fluids. From a practical standpoint it seems necessary that the two fluids either be rotating with a common rotational speed $\omega_1 = \omega_2$ (with possibly different mass densities) or else at least one of the fluids should be inviscid—otherwise, unwanted dynamical viscous effects at the free-boundary will be expected to interfere physically with the possibility of steady rigid rotation.

The volume of the incompressible drop is taken to be fixed

$$\text{volume}(\mathcal{D}_1) = V_1 = \frac{4}{3}\pi r_1^3 \quad (1.7)$$

for a given positive constant V_1 , where $r_1 > 0$ is the radius of a reference sphere with the same volume. It is also convenient to introduce a normalized angular speed $\hat{\omega}$ as

$$\hat{\omega} := \begin{cases} +[(\rho_1\omega_1^2 - \rho_2\omega_2^2)/8\sigma]^{1/2}r_1^{3/2} & \text{if } \rho_1\omega_1^2 \geq \rho_2\omega_2^2 \\ -[(\rho_2\omega_2^2 - \rho_1\omega_1^2)/8\sigma]^{1/2}r_1^{3/2} & \text{if } \rho_1\omega_1^2 < \rho_2\omega_2^2 \end{cases} \quad (1.8)$$

where r_1 is the radius of a reference sphere as in (1.7).

The total kinetic energy $T = \frac{1}{2} \int \rho|v|^2 dV$ for the rotating system is $T = T_1 + T_2 \equiv \frac{1}{2}\rho_1\omega_1^2 \int_{\mathcal{D}_1} r^2 dV + \frac{1}{2}\rho_2\omega_2^2 \int_{\mathcal{D}_2} r^2 dV = T_0 + T^*$ with

$$T_0 := \frac{1}{2}\rho_2\omega_2^2 \int_{\mathcal{D}_1 \cup \mathcal{D}_2} r^2 dV, \quad T^* := \frac{1}{2}(\rho_1\omega_1^2 - \rho_2\omega_2^2) \int_{\mathcal{D}_1} r^2 dV. \quad (1.9)$$

T_0 gives the kinetic energy that the system would have if the drop had the same density and rotational speed as the surrounding fluid (with T_0 independent of the interfacial free-boundary), while T^* represents an incremental kinetic energy associated with the free-boundary. Following D. Ross [11] we use the following nondimensionalized version \hat{T} of T^* as a measure of the kinetic energy for the system,

$$\hat{T} := \frac{|T^*|}{4\pi\sigma r_1^2}, \quad (1.10)$$

where $4\pi\sigma r_1^2$ is the potential energy of a reference sphere at rest with the radius r_1 as in (1.7), so that \hat{T} gives a measure of the kinetic energy as a fraction of the potential energy that the drop would have at rest. For a corresponding measure of the angular momentum we use

$$\hat{L} := \frac{2\hat{T}}{\hat{\omega}} = \frac{2\hat{\omega}}{\pi r_1^5} \int_{\mathcal{D}_1} r^2 dV \quad (1.11)$$

where the normalized angular speed $\hat{\omega}$ is given by (1.8).

2. Axisymmetric shapes

Consider now the special case of a smooth *axisymmetric* drop that occupies a time-independent domain $\mathcal{D} = \mathcal{D}_1$ which is rotationally symmetric about the axis of rotation. We introduce cylindrical coordinates (r, θ, z) with origin placed at the center of mass of the drop and with the cylindrical z -axis taken to coincide with the axis of rotation. Following Beer [2, 3] we seek axisymmetric drop shapes that are also symmetric across the equatorial plane $x_3 \equiv z = 0$. By Wente’s result it suffices to describe the “bottom” half of the symmetric drop in the negative half-space $z \leq 0$. The surface of the bottom half-drop is generated for $0 \leq \theta \leq 2\pi$ by the trace of the surface in an rz -plane which can be represented by the graph

$$z = Z(r) \quad \text{for } r_- \leq r \leq r_+ \quad (\text{with } r^2 = x_1^2 + x_2^2) \tag{2.1}$$

for suitable numbers r_- and r_+ with $0 \leq r_- < r_+$ and for a nonpositive-valued function $Z \leq 0$ satisfying $Z(r_+) = 0$.

The mean curvature of the axisymmetric surface generated by equation (2.1) can be given as (cf. Beer [3] or Gulliver[5])

$$H = \frac{1}{2} \left(\frac{dv}{dr} + \frac{v}{r} \right) \quad \text{with} \quad v(r) = \frac{Z'(r)}{\sqrt{1 + (Z'(r))^2}}. \tag{2.2}$$

The expression for H from (2.2) can be inserted into the left side of (1.3), and the resulting equation can be integrated to give

$$rv(r) = ar^4 + br^2 + c \tag{2.3}$$

with

$$a = \frac{\rho_1 \omega_1^2 - \rho_2 \omega_2^2}{8\sigma}, \quad b = \frac{p_0}{2\sigma}, \quad c = \text{integration constant}. \tag{2.4}$$

Inserting the expression for v from (2.2) into (2.3) yields directly

Theorem 2.1 (Beer [3], Gulliver [5]). *The surface obtained by rotating (2.1) about the z -axis satisfies the free-boundary equation (1.3) if and only if Z satisfies*

$$rZ'(r) = (ar^4 + br^2 + c)\sqrt{1 + (Z'(r))^2} \tag{2.5}$$

with constants a, b, c as in (2.4).

Regarding the constant c of integration, the case $c = 0$ leads to the spheroidal family studied by Beer [2, 3] for $a \geq 0$ and by Rosenthal [10] for $a < 0$, while the case $c \neq 0$ leads to the toroidal family studied by D. Ross [11] and Gulliver [5] (see also Rayleigh [9]).

Equation (2.5) can be solved for Z' and integrated to yield (with $Z(r_+) = 0$)

$$Z(r) \equiv Z(r; r_+, \mu, \lambda) = -r_+ \int_{r/r_+}^1 \frac{\psi(t, \mu, \lambda)}{\sqrt{t^2 - \psi(t, \mu, \lambda)^2}} dt \quad \text{for } 0 \leq r_- \leq r \leq r_+ \tag{2.6}$$

with

$$\psi(t, \mu, \lambda) \equiv \psi(t) := \mu(t^2 - 1)(t^2 - \lambda^2) + \frac{t^2 - \lambda}{1 - \lambda} \tag{2.7}$$

and with

$$0 \leq \lambda = \frac{r_-}{r_+} < 1, \tag{2.8}$$

where a, b, c of (2.5) have been written in terms of new parameters r_+, μ, λ as

$$a = \frac{\mu}{r_+^3}, \quad b = \frac{1-\mu}{r_+} + \frac{\lambda}{r_+} \left[\frac{1}{1-\lambda} - \mu\lambda \right], \quad \text{and} \quad c = -\lambda r_+ \left[\frac{1}{1-\lambda} - \mu\lambda \right]. \quad (2.9)$$

The integral in (2.6) can be expressed in terms of canonical hyperelliptic integrals, but equation (2.6) is convenient for our purposes. The parameter a can be eliminated between the relevant equations of (2.4) and (2.9) to give

$$\mu = \begin{cases} +(r_+/r_1)^3 \hat{\omega}^2 & \text{if } \rho_1 \omega_1^2 \geq \rho_2 \omega_2^2 \\ -(r_+/r_1)^3 \hat{\omega}^2 & \text{if } \rho_1 \omega_1^2 < \rho_2 \omega_2^2. \end{cases} \quad (2.10)$$

Negative values of $\mu < 0$ correspond to negative values of the angular speed $\hat{\omega} < 0$ as might occur in the case $\omega_1 = \omega_2$ if the outer fluid is denser than the drop fluid with $\rho_2 > \rho_1$.

The quantity $\lambda = r_-/r_+$ will serve as the primary parameter in the toroidal case with $0 < \lambda < 1$ and $c \neq 0$. In this case $Z(r_-) = Z(r_+) = 0$ for $0 < r_- < r_+$ and the drop does not intersect the z -axis of rotation. The spheroidal case occurs when both $\lambda = 0$ and $c = 0$, and in this case the drop intersects the z -axis with $Z'(0) = 0$. The quantity μ will serve as the primary parameter in the spheroidal case.

3. The spheroidal family

In this case $\lambda = 0$, $r_- = 0$, and the function ψ of (2.7) can be rewritten as

$$\psi(t, \mu, 0) = t\phi(t, \mu) \quad \text{with} \quad \phi(t, \mu) := (1 - \mu + \mu t^2)t. \quad (3.1)$$

Then (2.6) becomes

$$Z(r) \equiv Z(r; r_+, \mu) = -r_+ \int_{r/r_+}^1 \frac{\phi(t, \mu)}{\sqrt{1 - \phi(t, \mu)^2}} dt \quad \text{for } 0 = r_- \leq r \leq r_+, \quad (3.2)$$

where the positive parameter r_+ is the (outer) equatorial radius of the drop and will be determined below by the volume constraint in terms of μ . Proofs of the following Lemma 3.1 and Lemma 3.2 are given in the Appendix.

Lemma 3.1. *The integral giving $Z(r; r_+, \mu)$ in (3.2) exists for $0 \leq r/r_+ \leq 1$ for every μ satisfying*

$$-\frac{1}{2} < \mu < 4. \quad (3.3)$$

Now let $h(\mu)$ denote the integral (put $r = 0$ in (3.2))

$$h(\mu) := \int_0^1 \frac{\phi(t, \mu)}{\sqrt{1 - \phi(t, \mu)^2}} dt = \int_0^1 \frac{1 - \mu t^2}{\sqrt{1 + 2\mu - \mu(2 + \mu)t^2 + \mu^2 t^4}} dt \quad (3.4)$$

where the change of integration variable $t^2 \mapsto 1 - t^2$ has been used to obtain the last integral here, and then (3.2) yields $h(\mu) = -Z(0, \mu)/r_+$ for $-1/2 < \mu < 4$. The function h is smooth on the interval (3.3) and we find (see the Appendix for a proof)

Lemma 3.2. *The function $h(\mu)$ of (3.4) has precisely one root μ^* on the interval (3.3)*

$$h(\mu) = 0 \quad \text{for } \mu = \mu^*, \quad -\frac{1}{2} < \mu^* < 4 \quad (3.5)$$

with approximate value

$$\mu^* \doteq 2.32911. \tag{3.6}$$

The volume $V(r_+, \mu)$ of the drop obtained by revolving (2.1) and (3.2) about the z -axis is

$$V(r_+, \mu) = -4\pi \int_0^{r_+} Z(r; r_+, \mu)r \, dr = 2\pi r_+^3 \int_0^1 \frac{t^2 \phi(t, \mu)}{\sqrt{1 - \phi(t, \mu)^2}} \, dt \tag{3.7}$$

or equivalently (Rosenthal [10])

$$V(r_+, \mu) = \frac{2}{3} \pi r_+^3 \left[\frac{1 + (\mu - 1)h(\mu)}{\mu} \right] \tag{3.8}$$

where the last result follows from (3.4) and (3.7) upon integration of the identity

$$\frac{d}{dt} \sqrt{1 - \phi(t, \mu)^2} = \frac{[\mu - 1 - 3\mu t^2]\phi(t, \mu)}{\sqrt{1 - \phi(t, \mu)^2}}$$

over the interval $0 \leq t \leq 1$. The equatorial radius r_+ is determined in terms of μ by the volume constraint equation (1.7) along with (3.7) and (3.8) as

$$r_+ \equiv r_+(\mu) := \frac{r_1}{\sqrt[3]{H(\mu)}} \quad \text{for } -\frac{1}{2} < \mu \leq \mu^* \tag{3.9}$$

with

$$H(\mu) := \frac{3}{2} \int_0^1 \frac{t^2 \phi(t, \mu)}{\sqrt{1 - \phi(t, \mu)^2}} \, dt = \frac{1 + (\mu - 1)h(\mu)}{2\mu} \tag{3.10}$$

where $H(\mu) = 1 + O(\mu)$ as $\mu \rightarrow 0^+$ (because $h(\mu) = 1 - \mu + O(\mu^2)$). An argument similar to one employed in the proof (given in the Appendix) of Lemma 3.2 can be used to show that $H(\mu)$ is decreasing and positive for $-\frac{1}{2} < \mu \leq \mu^*$ (with $H(\mu^*) = 1/(2\mu^*) \doteq 0.21467$). Hence (3.9) and (3.10) determine a unique positive $r_+ = r_+(\mu) > 0$ (for $-1/2 < \mu \leq \mu^*$), and then the normalized angular speed $\hat{\omega}$ is given in terms of μ with (1.8) and (2.10). The angular momentum \hat{L} is computed with (1.11) along with the integral (cf. (3.2))

$$\begin{aligned} \int_{\mathcal{D}_1} r^2 \, dV &= -4\pi \int_0^{r_+} r^3 Z(r) \, dr = \pi r_+^5 \int_0^1 \frac{t^4 \phi(t, \mu)}{\sqrt{1 - \phi(t, \mu)^2}} \, dt \\ &= \pi r_+^5 \int_0^1 \frac{(1 - \mu t^2)(1 - t^2)^2}{\sqrt{(1 + 2\mu) - \mu(2 + \mu)t^2 + \mu^2 t^4}} \, dt \end{aligned} \tag{3.11}$$

where the change of integration variable $t^2 \mapsto 1 - t^2$ has been used to obtain the last integral in (3.11) which has a form that permits an easy numerical evaluation.

The graphs of the scaled distances $r_+(\mu)/r_1$ and $-Z(0, \mu)/r_+(\mu) = h(\mu)$ are indicated in Figure 1. The parameter values $0 \leq \mu \leq \mu^*$ yield the spheroidal shapes studied by Beer [2, 3] and D. Ross [11] with nonnegative angular speed $\hat{\omega}$, beginning with the sphere at $\mu = 0, \hat{\omega} = 0$ and progressing through oblate spheroidal shapes that bulge near the equator and flatten near the poles with *increasing* μ . The shapes become flatter with increasing μ until the polar diameter is sufficiently reduced so the shapes become biconcave with depressions at the poles, finally terminating with $Z(0) = 0$ at $\mu = \mu^*$ when the two poles touch at a certain angular speed $\hat{\omega}^* \doteq 0.7071$ with a final shape that is internally tangent to itself at the polar axis.

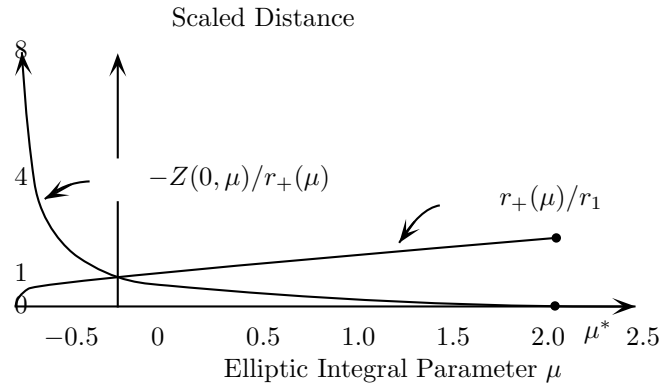


FIGURE 1. Spheroidal Drops

The parameter values $-0.5 < \mu < 0$ correspond to the typical case for which the outer medium is denser, and in this case the drop is referred to as a *bubble*; cf. Rosenthal [10] and D. Ross [11]. The bubble contracts at the equator and the polar diameter increases as the angular speed decreases with $\hat{\omega} \rightarrow -\infty$ as $\mu \rightarrow -1/2$. In this limit the bubble shape approaches that of a long cylindrical surface aligned and centered along the rotational axis with small corrections at the ends. Rosenthal [10] notes that the length of the bubble is asymptotically proportional to the four-thirds power of the angular speed $|\hat{\omega}|$ as $\hat{\omega} \rightarrow -\infty$ which provides an experimental approach for the determination of interfacial surface tensions; cf. Princen, Zia, and Mason [8].

The shapes of these various drops can be readily computed for fixed $-0.5 < \mu \leq \mu^*$ by a numerical calculation of the integral in (3.2); the integral is easily evaluated numerically using the second form of (A.1). Graphs of various typical drop cross-sections are included in Beer [3]; D. Ross [11]; Swiatecki [14]; and Tagg, Cammack, Croonquist, and Wang [15].

Angular speed $\hat{\omega}$ is plotted against angular momentum \hat{L} in Figure 2 for $-0.5 < \mu \leq \mu^*$. For the present spheroidal case, there is a minimum angular momentum $\hat{L}_{\min}^{\text{sph}} \doteq -0.66088$ achieved at a corresponding angular speed $\hat{\omega} \doteq -1.2853$. There are two distinct axisymmetric rotating bubbles, say $B'(\hat{L})$ and $B''(\hat{L})$, possessing a common angular momentum \hat{L} for any $\hat{L}_{\min}^{\text{sph}} < \hat{L} < 0$, with respective angular speeds $\hat{\omega}' < \hat{\omega}'' < 0$. The bubble $B''(\hat{L})$ approaches a sphere as $\hat{L} \rightarrow 0^-$ with $\mu \rightarrow 0^-$, while $B'(\hat{L})$ approaches a collapse onto the axis of rotation in the same limit $\hat{L} \rightarrow 0^-$ with angular speed $\hat{\omega}' \rightarrow -\infty$ as $\mu \rightarrow -0.5$. For $\hat{L}_{\min}^{\text{sph}} < \hat{L} < 0$ the bubbles $B'(\hat{L})$ and $B''(\hat{L})$ provide two different solutions to the “free bubble” problem that asks for a rotating bubble with specified volume as in (1.7) and specified angular momentum \hat{L} .

For $0 < \mu \leq \mu^*$ there is a terminal angular speed $\hat{\omega}^* = 1/\sqrt{2} \doteq 0.7071$ with corresponding angular momentum $\hat{L}^* \doteq 2.8506$ which is achieved at $\mu = \mu^* \doteq 2.3291$. There is also a maximum angular speed $\hat{\omega}_{\max}^{\text{sph}} \doteq 0.7538$ with corresponding $\hat{L} \doteq 1.9206$ at parameter value $\mu \doteq 1.7$. There are two distinct spheroidal rotating drops, say $\mathcal{D}'(\hat{\omega})$ and $\mathcal{D}''(\hat{\omega})$, with common angular speed $\hat{\omega}$ for any $\hat{\omega}^* \leq \hat{\omega} < \hat{\omega}_{\max}^{\text{sph}}$, with respective angular momenta $0 < \hat{L}' < \hat{L}''$. The drop $\mathcal{D}'(\hat{\omega})$ approaches a flattened sphere as $\hat{\omega} \rightarrow \hat{\omega}^*$ with $\mu \rightarrow 1^+$ and with corresponding $\hat{L} \doteq 1.259$. The other drop

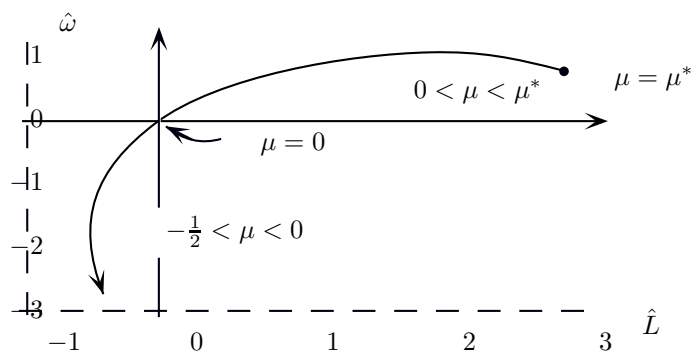


FIGURE 2. Spheroidal Drops: Angular Speed vs Angular Momentum

$\mathcal{D}''(\hat{\omega})$ approaches the terminal biconcave drop that is internally tangent to itself at the polar axis in the limit $\hat{\omega} \rightarrow \hat{\omega}^*$ with angular momentum $\hat{L} \rightarrow \hat{L}^*$ as $\mu \rightarrow \mu^*$. For $\hat{\omega}^* \leq \hat{\omega} < \hat{\omega}_{\max}^{\text{sph}}$ the drops $\mathcal{D}'(\hat{\omega})$ and $\mathcal{D}''(\hat{\omega})$ provide two solutions to the “driven drop” problem that asks for a rotating drop with specified volume as in (1.7) and specified angular speed $\hat{\omega}$.

4. The toroidal family

The toroidal case corresponds to a nonzero integration constant $c \neq 0$ in (2.5) which implies that the drop does not intersect the z -axis. The expression $t^2 - \psi(t)^2$ appearing in the denominator of the integral in (2.6) can be factored with (2.7) as $t^2 - \psi(t, \mu, \lambda)^2 = (1 - t^2)(t^2 - \lambda^2)[(1 - \lambda)^{-2} + [2\mu/(1 - \lambda)](t^2 - \lambda) - \mu^2(1 - t^2)(t^2 - \lambda^2)]$, and then (2.6), (2.7), and the change of integration variable $t^2 \mapsto 1 - t^2$ yield the equivalent expression for $Z(r; r_+, \mu, \lambda) \equiv Z(r)$

$$Z(r) = \int_0^{u(r/r_+)} \frac{-r_+ \left(\sqrt{1 - t^2}(1 - \mu t^2) + \lambda(\lambda\mu - (1 - \lambda)^{-1}) \frac{t^2}{\sqrt{1 - t^2}} \right) dt}{\sqrt{1 - \lambda^2 - t^2} \sqrt{2\mu + (1 - \lambda)^{-2} - \mu \left(\frac{2}{1 - \lambda} + \mu(1 - \lambda^2) \right) t^2 + \mu^2 t^4}} \quad (4.1)$$

with $u(t) := \sqrt{1 - t^2}$. A routine argument similar to that used in the proof of Lemma 3.1 can be applied to (4.1) to show that the integral for $Z(r)$ exists for $\lambda \leq r/r_+ \leq 1$ for every fixed $0 \leq \lambda < 1$ and for every μ satisfying

$$-\frac{1}{2} \left(\frac{1}{1 - \lambda} \right)^2 < \mu < \frac{4}{(1 - \lambda^2)(1 + \lambda)}, \quad (4.2)$$

where (4.2) reduces to the earlier (3.3) in the case $\lambda = 0$.

The function $Z(r)$ vanishes at the outer equatorial radius r_+ with $Z(r_+) = 0$. The positive number $r_- < r_+$ is the *inner* equatorial radius of the toroidal drop with $Z(r_-) \equiv Z(\lambda r_+) = 0$ (cf. (2.8)), characterized with (4.1) by the condition (cf. (3.5))

$$h(\mu, \lambda) = 0 \quad (4.3)$$

in terms of the function $h = h(\mu, \lambda)$ defined as

$$\begin{aligned}
 h(\mu, \lambda) &:= \int_{\lambda}^1 \frac{\psi(t, \mu, \lambda)}{\sqrt{t^2 - \psi(t, \mu, \lambda)^2}} dt \\
 &= \int_0^{\sqrt{1-\lambda^2}} \frac{\left(\sqrt{1-t^2}(1-\mu t^2) + \lambda(\lambda\mu - (1-\lambda)^{-1})\frac{t^2}{\sqrt{1-t^2}}\right) dt}{\sqrt{1-\lambda^2-t^2}\sqrt{2\mu + (1-\lambda)^{-2} - \mu\left(\frac{2}{1-\lambda} + \mu(1-\lambda^2)\right)t^2 + \mu^2 t^4}}
 \end{aligned}
 \tag{4.4}$$

for $0 \leq \lambda < 1$ and for all μ satisfying (4.2). Note that the present $h(\mu, \lambda)$ reduces to the earlier $h(\mu)$ of (3.4) in the special case $\lambda = 0$. A direct calculation from (4.4) yields $\partial h(\mu, \lambda)/\partial \mu < 0$ (cf. (A.17)), and then an argument related to that used in the proof of Lemma 3.2 shows that (4.3) and (4.4) determine $\mu = \mu^{**}(\lambda)$ in terms of λ ,

$$\mu = \mu^{**}(\lambda) \quad \text{for } 0 \leq \lambda < 1.
 \tag{4.5}$$

The value of the function $\mu^{**}(\lambda)$ coincides at $\lambda = 0$ with the earlier value of Lemma 3.2,

$$\mu^{**}(0) = \mu^* \doteq 2.32911
 \tag{4.6}$$

in the case $\lambda = 0$. The graph of $\mu^{**}(\lambda)$ is indicated in Figure 3 where it is seen that $\mu = \mu^{**}(\lambda)$ decreases initially for increasing small values of $\lambda > 0$. The initial slope is infinite (the graph possesses an initially vertical slope that is tangent to the μ -axis at $\lambda = 0$), but this cannot be detected in Figure 3 because of the scale used there and the fact that the slope has only a mild singularity behaving like $\ln \lambda$ as $\lambda \rightarrow 0^+$ (cf. (A.32)).

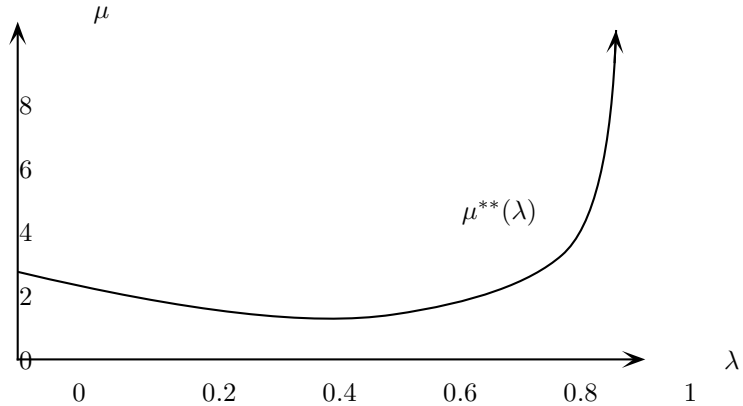


FIGURE 3. Toroidal Drops: Elliptic Integral Parameters μ, λ

The volume $V(\lambda)$ of the drop obtained by revolving (2.1) and (4.1) about the z -axis is (cf. (2.8), (4.5))

$$\begin{aligned}
 V(r_+, \lambda) &= -4\pi \int_{r_-}^{r_+} Z(r; r_+, \mu^{**}(\lambda), \lambda) r dr \\
 &= 2\pi r_+^3 \int_{\lambda}^1 \frac{(t^2 - \lambda^2)\psi(t, \mu^{**}(\lambda), \lambda)}{\sqrt{t^2 - \psi(t, \mu^{**}(\lambda), \lambda)^2}} dt.
 \end{aligned}
 \tag{4.7}$$

The outer equatorial radius r_+ is now fixed in terms of λ by the volume constraint (1.7) along with (4.7) as

$$r_+ \equiv r_+[\lambda] := \frac{r_1}{\sqrt[3]{H^*(\lambda)}} \quad \text{for } 0 \leq \lambda < 1 \tag{4.8}$$

with

$$H^*(\lambda) := \frac{3}{2} \int_{\lambda}^1 \frac{(t^2 - \lambda^2)\psi(t, \mu^{**}(\lambda), \lambda)}{\sqrt{t^2 - \psi(t, \mu^{**}(\lambda), \lambda)^2}} dt \quad \text{for } 0 \leq \lambda < 1, \tag{4.9}$$

and then the inner equatorial radius is given as

$$r_- = \lambda r_+[\lambda]. \tag{4.10}$$

From (2.9) and (4.8) follows $a = \mu^{**}(\lambda)H^*(\lambda)/r_+^3 > 0$, which with (2.4) yields $\rho_1\omega_1^2 > \rho_2\omega_2^2$. Hence the fluid of the drop must “dominate” the surrounding fluid in the toroidal case: the analogue of the spheroidal bubble with $\rho_1\omega_1^2 \leq \rho_2\omega_2^2$ cannot occur in the toroidal case.

The shape of the drop is determined by the function $Z(r; r_+[\lambda], \mu^{**}(\lambda), \lambda) = Z(r)$ of (4.1), where this function is readily computed for fixed $0 \leq \lambda < 1$ by a numerical evaluation of the integral in (4.1) evaluated for $\mu = \mu^{**}(\lambda)$ and $r_+ = r_+[\lambda]$. The angular momentum is given with (1.11) using (cf. (4.1), (4.10))

$$\begin{aligned} \int_{\mathcal{D}_1} r^2 dV &= -4\pi \int_{r_-}^{r_+} r^3 Z(r) dr \\ &= \pi r_+[\lambda]^5 \int_{\lambda}^1 \frac{(t^4 - \lambda^4)\psi(t, \mu^{**}(\lambda), \lambda)}{\sqrt{t^2 - \psi(t, \mu^{**}(\lambda), \lambda)^2}} dt, \end{aligned} \tag{4.11}$$

where the last integral can be recast in a computationally preferred form through the change of integration variable $t^2 \mapsto 1 - t^2$.

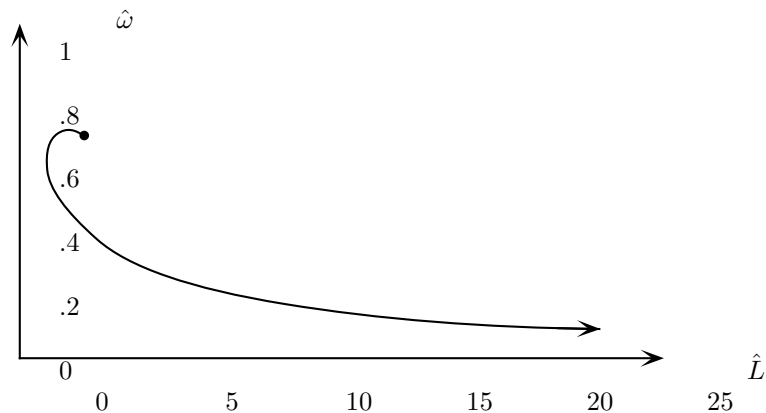


FIGURE 4. Toroidal Drops: Angular Speed vs Angular Momentum

The initial toroidal parameter value $\lambda = 0$ corresponds to a terminal spheroidal drop for which the two poles touch with $Z(0) = 0$ and for which the drop is internally tangent to itself, with spheroidal parameter $\mu = \mu^* \doteq 2.32911$ as discussed in §3. With increasing $\lambda > 0$ the previously internally tangent spheroidal drop (for $\lambda = 0$)

separates from the rotational axis and forms a toroidal shape for $0 < \lambda < 1$. The equatorial radius of the resulting toroidal drop increases without bound and the cross-section of the torus becomes approximately circular as the parameter $\lambda \rightarrow 1^-$. Angular speed is plotted against angular momentum for the toroidal shapes in Figure 4. There is a maximum toroidal angular speed $\hat{\omega}_{\max}^{\text{tor}} \doteq 0.72718$ with corresponding angular momentum $\hat{L} \doteq 2.2963$ at parameter value $\lambda \doteq 0.03164$, and there is a minimum toroidal angular momentum $\hat{L}_{\min}^{\text{tor}} \doteq 1.679458$ with corresponding angular speed $\hat{\omega} \doteq 0.60498$ at parameter value $\lambda \doteq 0.24945$.

5. The bifurcation

Plateau [7] devised and performed a version of a rotating drop experiment in which a viscous liquid drop is driven by an enclosed rotating spindle while being immiscibly levitated in another surrounding liquid with approximately the same density but with a much smaller viscosity. The surrounding liquid supports the rotating drop so as to cancel most of the effects of the earth's gravity. In his experiments Plateau observed axisymmetric shapes symmetric about the rotational axis of the drop, beginning with a sphere when the rotation speed is zero. For small positive rotational speeds Plateau's axisymmetric shapes were oblate spheroids that bulge near the equator and flatten near the poles. The shapes became flatter with increasing rotational speed until the polar thickness contracted and the shapes became biconcave with depressions at the poles, similar to the shapes of §3 for $\hat{\omega} \geq 0$.

Plateau also observed *bubbles* similar to those of §3 for $\hat{\omega} < 0$ and he observed other shapes as well, including axisymmetric toroidal profiles that did not meet the axis of rotation, similar to the shapes of §4. The latter toroidal shapes were obtained by driving the rotating spindle harder with a larger angular speed and momentum. The nature of the presumed bifurcation from the axisymmetric spheroidal to toroidal shapes has been the subject of some uncertainty with different authors asserting that a bifurcation occurs either with an increase in angular momentum, an increase in angular speed, or an increase in the parameter μ of (2.10). Rayleigh [9] states that the toroidal shapes should arise at “*higher rotations*”, while Swiatecki [14] asserts that if a (liquid) “*globe with surface tension is rotated, it flattens at first into an oblate pseudospheroid which, with increasing angular momentum, eventually goes over into a torus.*” Chandrasekhar [4, p. 62] remarks on “*the emergence of a sequence of toroidal figures*” for parameter values $\mu > 2.3291$. These statements are generally open to ambiguous interpretation and indeed Tagg, Cammack, Croonquist, and Wang [15] note simply that it “*is less certain where the toroidal shapes arise*”. We find that the bifurcation from spheroidal to toroidal shapes which occurs at $\hat{\omega} = \hat{\omega}^* = 1/\sqrt{2}$ (and $\hat{L} = \hat{L}^* \doteq 2.8506$) leads initially to a *decrease* in angular momentum, a decrease in the parameter μ , and an increase in angular speed. After the bifurcation as one proceeds further along the toroidal family, the angular momentum and the parameter μ eventually increase without bound while the angular speed eventually decreases toward zero.

The toroidal and spheroidal families connect at the bifurcation point with a common slope in the $(\hat{L}, \hat{\omega})$ -plane as indicated in Figure 5. The resulting bifurcation slope can be computed in terms of the derivative $h'(\mu)$ at $\mu = \mu^*$ (cf. (3.4), (A.3)) along with

the value at $\mu = \mu^*$ of the function

$$J(\mu) := 2 \int_0^1 t \sqrt{1 - \phi(t, \mu)^2} dt, \tag{5.1}$$

as indicated in Theorem 5.1 which is proved in the Appendix and which complements a related convergence result of Gulliver [5].

Theorem 5.1. *The spheroidal and toroidal axisymmetric shapes connect tangentially in the $(\hat{L}, \hat{\omega})$ -plane at the bifurcation point $(\hat{L}^*, \hat{\omega}^*)$ with common slope*

$$\begin{aligned} \left. \frac{d\hat{\omega}}{d\hat{L}} \right|_{(\hat{L}^*, \hat{\omega}^*)} &= \frac{27(\mu^*/4)^{4/3}(\mu^* - 1)h'(\mu^*)}{6(2\mu^* + 1) + \mu^*(\mu^* - 1)(-h'(\mu^*))[\mu^* - 1 + 21\mu^*J(\mu^*)]} \\ &\doteq -0.070757 \end{aligned} \tag{5.2}$$

where μ^* is the root of $h(\mu)$ of Lemma 3.2.

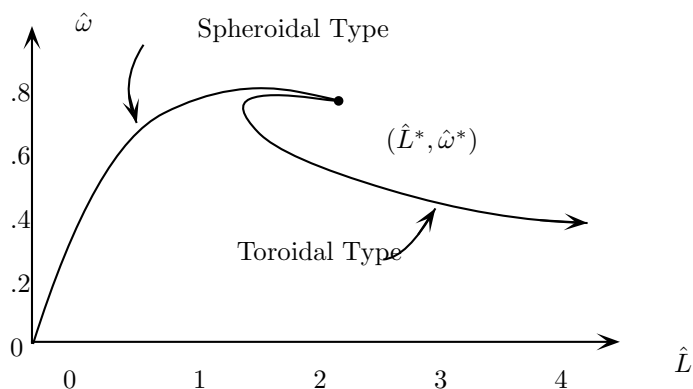


FIGURE 5. Angular Speed vs Angular Momentum

The axisymmetric family which begins with the sphere at $(\hat{L}, \hat{\omega}) = (0, 0)$ bifurcates at $(\hat{L}, \hat{\omega}) = (\hat{L}^*, \hat{\omega}^*)$ from spheroidal to toroidal shapes as indicated in Figure 5 where angular speed is plotted versus angular momentum for the toroidal family superimposed on a similar plot for the spheroidal family with $\hat{L} > 0, \hat{\omega} > 0$. The bifurcation results in an initial decrease in angular momentum and a corresponding increase in angular speed. The problem of the *driven drop* (specified angular speed) has four distinct axisymmetric solutions for any specified angular speed $\hat{\omega}$ in the range $\hat{\omega}^* < \hat{\omega} < \hat{\omega}_{\max}^{\text{tor}}$, two solutions of toroidal type and two of spheroidal type. There are three axisymmetric solutions to the driven drop problem in the case $\hat{\omega} = \hat{\omega}^*$, consisting of the bifurcation solution along with one toroidal and one spheroidal solution each distinct from the bifurcation solution. The *free drop* problem (specified angular momentum) has three axisymmetric solutions for any specified angular momentum \hat{L} in the range $\hat{L}_{\min}^{\text{tor}} < \hat{L} < \hat{L}^*$, one solution of spheroidal type and two of toroidal type. For large angular momentum $\hat{L} > \hat{L}^*$, the free drop problem has only one axisymmetric solution and it is of toroidal type. Nothing is implied here regarding the stability or instability of these various solutions.

The case in which the surrounding fluid is *compressible* is discussed in a forthcoming work.

Acknowledgments. We thank Robert Finn for the reference to Laugwitz [6], Roland Bulirsch for making available to us a copy of the reference Beer [3], Robert Gulliver for useful remarks, and we particularly thank William A. Harris, Jr. for encouragement and early discussions of techniques.

A. Appendix

Proof of Lemma 3.1. The change of integration variable $t^2 \mapsto 1 - t^2$ yields with (3.1)

$$\int_{r/r_+}^1 \frac{\phi(t, \mu)}{\sqrt{1 - \phi(t, \mu)^2}} dt = \int_0^{u(r/r_+)} \frac{1 - \mu t^2}{\sqrt{(1 + 2\mu) - \mu(2 + \mu)t^2 + \mu^2 t^4}} dt \quad (\text{A.1})$$

with $u(t) := \sqrt{1 - t^2}$, and a routine calculation shows that the second integral here exists for the stated values of r and μ . Indeed the function $(1 + 2\mu) - \mu(2 + \mu)\tau + \mu^2\tau^2$ has (for $\mu \neq 0$) a minimum point at $\tau = (2 + \mu)/2\mu$ with minimum value $\mu(4 - \mu)/4 \leq (1 + 2\mu) - \mu(2 + \mu)\tau + \mu^2\tau^2$ for all real τ . Replacing τ with t^2 yields

$$(1 + 2\mu) - \mu(2 + \mu)t^2 + \mu^2 t^4 > 0 \quad \text{for } 0 \leq t \leq 1 \quad (\text{A.2})$$

if $0 < \mu < 4$. On the other hand if $-1/2 < \mu \leq 0$, an examination of the signs of the coefficients of the quadratic $(1 + 2\mu) - \mu(2 + \mu)\tau + \mu^2\tau^2$ shows that (A.2) holds also in this case. A compactness argument then shows that the integrand function in the second integral of (A.1) is uniformly bounded for $0 \leq t \leq 1$ for each fixed μ satisfying (3.3), and this completes the proof of the lemma. \square

Proof of Lemma 3.2. The function h of (3.4) is smooth on the interval (3.3) with

$$h'(\mu) = - \int_0^1 \frac{1}{[(1 + 2\mu) - \mu(2 + \mu)t^2 + \mu^2 t^4]^{3/2}} dt \quad \text{for } -\frac{1}{2} < \mu < 4, \quad (\text{A.3})$$

so h is a decreasing function with $h'(\mu) < 0$. We now show the result

$$h(\mu) \rightarrow -\infty \quad \text{as } \mu \rightarrow 4^-, \quad (\text{A.4})$$

and this will prove the existence of a unique root μ^* on the interval (3.3), with $0 < \mu^* < 4$ because $h(0) = +1$ as is seen by a direct evaluation of the integral in (3.4) for $\mu = 0$. For the proof of (A.4) write $h(\mu) = h_1(\mu) + h_2(\mu)$ with (cf. (3.4))

$$\begin{aligned} h_1(\mu) &= \int_0^{3/4} \frac{1 - \mu t^2}{\sqrt{1 + 2\mu - \mu(2 + \mu)t^2 + \mu^2 t^4}} dt, \\ h_2(\mu) &= \int_{3/4}^1 \frac{1 - \mu t^2}{\sqrt{1 + 2\mu - \mu(2 + \mu)t^2 + \mu^2 t^4}} dt. \end{aligned} \quad (\text{A.5})$$

In the following we impose, without loss of generality, the restriction $2 \leq \mu < 4$. For such μ and for $0 \leq t \leq 3/4$ one readily has $1 - \mu t^2 \leq 1$ and $1 + 2\mu - \mu(2 + \mu)t^2 + \mu^2 t^4 \geq 1$, so h_1 is bounded with $|h_1(\mu)| \leq \int_0^{3/4} 1 dt = 3/4$. Similarly for $3/4 \leq t \leq 1$ there hold $1 - \mu t^2 \leq -1/8$ and $1 + 2\mu - \mu(2 + \mu)t^2 + \mu^2 t^4 \leq 2[(4 - \mu) + (3 - 4t^2)^2] \leq 2[(4 - \mu) + 16(\sqrt{3} - 2t)^2]$, so for h_2 , (A.5) yields $8\sqrt{2}h_2(\mu) \leq - \int_{3/4}^1 [(4 - \mu) + 16(\sqrt{3} - 2t)^2]^{-1/2} dt$. This last integral can be evaluated, and it becomes unbounded like $\ln(1/\sqrt{4 - \mu})$ as $\mu \rightarrow 4^-$. Hence $h_2(\mu) \rightarrow -\infty$ as $\mu \rightarrow 4^-$, and then the result (A.4) follows directly from this last result along with $h = h_1 + h_2$ and the boundedness of h_1 . This completes the proof of the existence of a unique root μ^* for h in the interval (3.3), satisfying

$0 < \mu^* < 4$. Newton's method can be used to solve the equation $h(\mu) = 0$, yielding the approximate value of (3.6). \square

Proof of Theorem 5.1. The angular speeds and momentums are obtained from (1.8), (1.11), (2.7), (2.10), (3.1), (4.6), (4.11) in the toroidal and spheroidal cases as

$$\text{toroidal case: } \begin{cases} \hat{\omega} = f(\mu, \lambda)|_{\mu=\mu^{**}(\lambda)} \\ \hat{L} = g(\mu, \lambda)|_{\mu=\mu^{**}(\lambda)} \end{cases} \quad \text{for } 0 \leq \lambda < 1, \quad (\text{A.6})$$

and

$$\text{spheroidal case: } \begin{cases} \hat{\omega} = f(\mu, 0) \\ \hat{L} = g(\mu, 0) \end{cases} \quad \text{for } 0 \leq \mu \leq \mu^*, \quad (\text{A.7})$$

where

$$f(\mu, \lambda) := \left[\frac{3}{2} \mu I_2(\mu, \lambda) \right]^{1/2}, \quad g(\mu, \lambda) := 2 \left(\frac{2}{3} \right)^{7/6} \mu^{1/2} I_2(\mu, \lambda)^{-7/6} I_4(\mu, \lambda) \quad (\text{A.8})$$

with

$$I_2(\mu, \lambda) := \int_{\lambda}^1 \frac{(t^2 - \lambda^2) \psi(t, \mu, \lambda)}{\sqrt{t^2 - \psi(t, \mu, \lambda)^2}} dt, \quad I_4(\mu, \lambda) := \int_{\lambda}^1 \frac{(t^4 - \lambda^4) \psi(t, \mu, \lambda)}{\sqrt{t^2 - \psi(t, \mu, \lambda)^2}} dt \quad (\text{A.9})$$

for suitable values of $0 < \mu \leq \mu^*$, $0 \leq \lambda < 1$, and where $\mu^{**}(\lambda)$ is the function of (4.5). The slope in the $(\hat{L}, \hat{\omega})$ -plane along the toroidal family is obtained from (A.6) as $d\hat{\omega}/d\hat{L} = [d\hat{\omega}/d\lambda]/[d\hat{L}/d\lambda]$ which gives for the toroidal bifurcation slope

$$\left. \frac{d\hat{\omega}}{d\hat{L}} \right|_{\text{tor}} = \lim_{\lambda \rightarrow 0^+} \left[\frac{f_{\lambda}(\mu, \lambda) + f_{\mu}(\mu, \lambda)(d\mu^{**}/d\lambda)}{g_{\lambda}(\mu, \lambda) + g_{\mu}(\mu, \lambda)(d\mu^{**}/d\lambda)} \Big|_{\mu=\mu^{**}(\lambda)} \right], \quad (\text{A.10})$$

and similarly for the spheroidal family from (A.7)

$$\left. \frac{d\hat{\omega}}{d\hat{L}} \right|_{\text{sph}} = \lim_{\mu \rightarrow \mu^*} \frac{f_{\mu}(\mu, 0)}{g_{\mu}(\mu, 0)} = \frac{f_{\mu}(\mu^*, 0)}{g_{\mu}(\mu^*, 0)} \quad (\text{A.11})$$

where the subscripts on f , g denote partial derivatives.

In the following we use the identities

$$3\mu I_2(\mu, 0) = 1 + (\mu - 1)h(\mu), \quad (\text{A.12})$$

$$3\mu I_4(\mu, 0) = J(\mu) + (\mu - 1)I_2(\mu, 0) \quad \text{for } -0.5 < \mu < 4,$$

where the first identity here has already been noted (cf. (3.7)–(3.8)) and the second follows upon integration of the identity

$$\frac{d}{dt} \left[t^2 \sqrt{1 - \phi(t, \mu)^2} \right] = 2t \sqrt{1 - \phi(t, \mu)^2} + \frac{t^2 [\mu - 1 - 3\mu t^2] \phi(t, \mu)}{\sqrt{1 - \phi(t, \mu)^2}}$$

over the interval $0 \leq t \leq 1$. The identities (A.12) imply that the values $I_2(\mu, \lambda)$, $I_4(\mu, \lambda)$ are positive at the bifurcation point and by continuity these values are positive locally everywhere near the bifurcation point. Similarly the relevant derivatives f_{μ} , f_{λ} , g_{μ} , g_{λ} are seen to exist near the bifurcation point. The first identity of (A.12) can be differentiated and used with the definition of f in (A.8)–(A.9) to give (note $h(\mu^*) = 0$ from Lemma 3.2)

$$f(\mu^*, 0) = \frac{1}{\sqrt{2}}, \quad f_{\mu}(\mu^*, 0) = \frac{(\mu^* - 1)h'(\mu^*)}{(2\sqrt{2})}, \quad (\text{A.13})$$

and similarly the second identity of (A.12) can be used to yield

$$g(\mu^*, 0) = \frac{2^{13/6}[\mu^* - 1 + 3\mu^* J(\mu^*)]}{9(\mu^*)^{1/3}}, \quad (\text{A.14})$$

$$g_\mu(\mu^*, 0) = \frac{2^{7/6}[6(2\mu^* + 1) - \mu^*(\mu^* - 1)h'(\mu^*)(\mu^* - 1 + 21\mu^* J(\mu^*))]}{27(\mu^*)^{4/3}}.$$

From (A.3), (5.1), (A.13), and (A.14)

$$f_\mu(\mu^*, 0) < 0, \quad g_\mu(\mu^*, 0) > 0, \quad (\text{A.15})$$

and then the stated conclusions of the theorem follow directly from (A.6)–(A.11), (2.7), and (A.13)–(A.15) using the result of the following lemma.

Lemma . *The function μ^{**} of (4.3)–(4.5) is of class \mathcal{C}^1 for $0 < \lambda < 1$, with first derivative satisfying*

$$\lim_{\lambda \rightarrow 0^+} \frac{d\mu^{**}(\lambda)}{d\lambda} = -\infty. \quad (\text{A.16})$$

Proof. A routine calculation from (2.7), (4.3), and (4.4) shows that $h(\mu, \lambda)$ is differentiable with respect to μ with

$$\frac{\partial h(\mu, \lambda)}{\partial \mu} = - \int_{\lambda}^1 \frac{t^2(1-t^2)(t^2-\lambda^2)}{[t^2-\psi(t, \mu, \lambda)]^{3/2}} dt \quad (\text{A.17})$$

where the last integral exists and yields

$$\lim_{\lambda \rightarrow 0^+} \left[\frac{\partial h(\mu, \lambda)}{\partial \mu} \Big|_{\mu=\mu^{**}(\lambda)} \right] = - \int_0^1 \frac{t(1-t^2)}{[1-\phi(t, \mu^*)]^{3/2}} dt < 0. \quad (\text{A.18})$$

This last limit exists and the limiting value is finite and negative. (Note that $\mu^{**}(\lambda) \rightarrow \mu^*$ as $\lambda \rightarrow 0^+$.) An attempt to routinely differentiate $h(\mu, \lambda)$ with respect to λ fails because the integrand $\psi/\sqrt{t^2-\psi^2}$ in (4.4) behaves like $1/\sqrt{t-\lambda}$ near $t = \lambda$ and is infinite at $t = \lambda$. Hence to check the λ -differentiability of h near $\lambda = 0$ we use (4.4) to write $h(\mu, \lambda) = h_1(\mu, \lambda) + h_2(\mu, \lambda)$ for $0 \leq \lambda < 1$ with

$$h_1(\mu, \lambda) := \int_{1/4}^1 \frac{\psi(t, \mu, \lambda)}{\sqrt{t^2 - \psi(t, \mu, \lambda)^2}} dt, \quad (\text{A.19})$$

$$h_2(\mu, \lambda) := \int_{\lambda}^{1/4} \frac{\psi(t, \mu, \lambda)}{\sqrt{t^2 - \psi(t, \mu, \lambda)^2}} dt.$$

The function h_1 is easily seen to be differentiable with

$$\frac{\partial h_1(\mu, \lambda)}{\partial \lambda} = \int_{1/4}^1 \frac{t^2 \partial \psi(t, \mu, \lambda) / \partial \lambda}{[t^2 - \psi(t, \mu, \lambda)^2]^{3/2}} dt \quad (\text{A.20})$$

where the integral exists for all relevant values of μ and λ . From (2.7), (A.20), and the factorization of $t^2 - \psi^2$ mentioned prior to (4.1) follows

$$\lim_{\lambda \rightarrow 0^+} \frac{\partial h_1(\mu, \lambda)}{\partial \lambda} = - \int_{1/4}^1 \frac{dt}{t\sqrt{1-t^2} [1 + 2\mu t^2 - \mu^2 t^2(1-t^2)]^{3/2}} < 0. \quad (\text{A.21})$$

Turning now to h_2 in (A.19), we write

$$h_2(\mu, \lambda) = \int_{\lambda}^{1/4} \frac{A(t, \mu, \lambda)}{\sqrt{t - \lambda}} dt \quad (\text{A.22})$$

with

$$A(t, \mu, \lambda) := \begin{cases} \psi(t, \mu, \lambda) \sqrt{\frac{t - \lambda}{t^2 - \psi(t, \mu, \lambda)^2}} & \text{for } \lambda < t \leq 1/4, \\ -\frac{\sqrt{\lambda/2}}{\sqrt{(1 - \lambda^2)[(1 - \lambda)^{-2} - 2\mu\lambda]}} & \text{for } t = \lambda. \end{cases} \quad (\text{A.23})$$

We are here restricting consideration to $0 < \lambda < 1/4$ because we are interested in the limiting behavior as $\lambda \rightarrow 0^+$. However, the present approach can be modified to handle any $0 < \lambda < 1$. The change of integration variable $t - \lambda \mapsto t$ in (A.22) yields

$$h_2(\mu, \lambda) = \int_0^{1/4 - \lambda} \frac{A(t + \lambda, \mu, \lambda)}{\sqrt{t}} dt$$

which is seen to be differentiable for $0 < \lambda < 1/4$ with

$$\frac{\partial h_2(\mu, \lambda)}{\partial \lambda} = -\frac{A(1/4, \mu, \lambda)}{\sqrt{(1/4) - \lambda}} + \int_0^{1/4 - \lambda} \frac{A_t(t + \lambda, \mu, \lambda) + A_\lambda(t + \lambda, \mu, \lambda)}{\sqrt{t}} dt \quad (\text{A.24})$$

for $0 < \lambda < 1/4$, where the subscripts on A in the last integrand denote partial derivatives. The first term on the right side of (A.24) is regular near $\lambda = 0$ with (cf. (A.23), (2.7))

$$\begin{aligned} \lim_{\lambda \rightarrow 0^+} \frac{A(1/4, \mu, \lambda)}{\sqrt{(1/4) - \lambda}} &= \frac{\psi(t, \mu, 0)}{\sqrt{t^2 - \psi(t, \mu, 0)^2}} \Big|_{t=1/4} \\ &= \frac{16 - 15\mu}{\sqrt{15}\sqrt{(16 + 5\mu)(16 - 3\mu)}}. \end{aligned} \quad (\text{A.25})$$

One sees with (A.23) that the integral on the right side of (A.24) exists for fixed $0 < \lambda < 1/4$ (cf. (A.26)–(A.27) below), but we shall now show that this integral becomes unbounded as $\lambda \rightarrow 0^+$ (see (A.29) below).

The quantity $A_t + A_\lambda$ appearing in the integrand on the right side of (A.24) can be computed with (2.7) and (A.23) to give

$$(A_t + A_\lambda)(t, \mu, \lambda) = \frac{t(t - \lambda)^{3/2}}{[t^2 - \psi(t, \mu, \lambda)^2]^{3/2}} B(t, \mu, \lambda) \quad (\text{A.26})$$

with

$$B(t, \mu, \lambda) = 3\mu t^3 + [(1 - \lambda)^{-2} + \mu\lambda]t^2 + [(1 - \lambda)^{-2} - \mu]t + [\mu\lambda - (1 - \lambda)^{-1}]. \quad (\text{A.27})$$

We are preparing to take the limit as $\lambda \rightarrow 0^+$, and in this case the function B is uniformly negative on the relevant domain; for example, one has

$$B(t, \mu, \lambda) \leq -\frac{1}{4} \quad \text{for } 0 \leq t \leq \frac{1}{4}, \quad 0 \leq \lambda \leq \frac{1}{10}, \quad (\text{A.28})$$

uniformly for all μ near μ^* . Hence, with (A.26), (A.28), and the factorization of $t^2 - \psi^2$ mentioned prior to (4.1), we have the existence of a fixed positive constant $\kappa > 0$ for

which

$$\frac{A_t(t + \lambda, \mu, \lambda) + A_\lambda(t + \lambda, \mu, \lambda)}{\sqrt{t}} \leq -2\kappa \frac{(t + \lambda)t}{t^{3/2}(t + 2\lambda)^{3/2}}$$

uniformly for $0 \leq t \leq \frac{1}{4} - \lambda$, $0 \leq \lambda \leq \frac{1}{10}$ and for all relevant μ (near μ^*). Integration of this last inequality using $(t + \lambda)/(t + 2\lambda) \geq 1/2$ yields

$$\begin{aligned} \int_0^{\frac{1}{4}-\lambda} \frac{A_t(t + \lambda, \mu, \lambda) + A_\lambda(t + \lambda, \mu, \lambda)}{\sqrt{t}} dt &\leq -\kappa \int_0^{\frac{1}{4}-\lambda} \frac{dt}{\sqrt{t(t + 2\lambda)}} \\ &= -\kappa \ln \left(\frac{1 + \sqrt{1 - 16\lambda^2}}{4\lambda} \right) \end{aligned} \quad (\text{A.29})$$

for $0 < \lambda \leq \frac{1}{10}$. This proves that the last term on the right side of (A.24) becomes unbounded as $\lambda \rightarrow 0^+$.

Directly from (A.21), (A.24), (A.25), (A.29), and $h = h_1 + h_2$ follows

$$\lim_{\lambda \rightarrow 0^+} \frac{\partial h(\mu, \lambda)}{\partial \lambda} = -\infty. \quad (\text{A.30})$$

Implicit differentiation of (4.3)–(4.5) shows that μ^{**} is of class \mathcal{C}^1 with

$$\frac{d\mu^{**}(\lambda)}{d\lambda} = - \frac{\partial h(\mu, \lambda)/\partial \lambda}{\partial h(\mu, \lambda)/\partial \mu} \Big|_{\mu=\mu^{**}(\lambda)} \quad \text{for } 0 < \lambda < 1, \quad (\text{A.31})$$

and the result (A.16) follows from (A.18), (A.30), and (A.31). \square

The method of proof of this last lemma actually yields the stronger result

$$\frac{d\mu^{**}(\lambda)}{d\lambda} \sim \ln \lambda \quad \text{as } \lambda \rightarrow 0^+. \quad (\text{A.32})$$

The numerical value $-0.070757 \dots$ in (5.2) follows from the first line there by numerical evaluations of the relevant integrals for $h'(\mu^*)$ and $J(\mu^*)$.

References

1. A. D. Alexandrov, *Uniqueness theorems for surfaces in the large*, Vestnik Leningrad Univ. **13**(19) (1958), 5–8; Trans. Amer. Math. Soc. (2), **21** (1958), 412–416.
2. A. Beer, Pogg. Ann., **96** (1855), 210.
3. ———, *Einleitung in der mathematische Theorie der Elasticität und Capillarität*, part 2, A. Gissen Verlag, Leipzig, 1869.
4. S. Chandrasekhar, *The stability of a rotating liquid drop*, Proc. Roy. Soc. London Ser. A **286** (1965), 1–26.
5. R. Gulliver, *Tori of prescribed mean curvature and the rotating drop*, Soc. Math. France Astérisque, **118** (1984), 167–179.
6. D. Laugwitz, *Differential and Riemannian Geometry*, English translation, Academic Press, New York and London, 1965.
7. J. A. F. Plateau, *Mémoire sur les phénomènes que présente une masse liquide libre et soustraite à l'action de la pesanteur*, Mémoires de l'Acad. Bruxelles **16** (1843), 1–35; English translation *Experimental and theoretical researches on the figures of equilibrium of a liquid mass withdrawn from the action of gravity*, The Annual Report of the Board of Regents of the Smithsonian Institute, 1863, Government Printing Office, Washington D.C., 207–225.
8. H. M. Princen, I. Y. Z. Zia, and S. G. Mason, *Measurement of interfacial tension from the shape of a rotating drop*, J. Colloid Interface Sci. **23** (1967), 99–107.
9. Lord Rayleigh, *The equilibrium of revolving liquid under capillary force*, Philos. Mag. (6) **28** (1914), 161–170.

10. D. K. Rosenthal, *The shape and stability of a bubble at the axis of a rotating liquid*, J. Fluid Mech. **12** (1962), 358–366.
11. D. K. Ross, *The shape and energy of a revolving liquid mass held together by surface tension*, Austral. J. Phys. **21** (1968), 823–835.
12. J. E. Ross and D. R. Smith, *On an ODE model for narrow-necked rotating liquid drops*, Adv. in Appl. Math., to appear.
13. D. R. Smith, *An Introduction to Continuum Mechanics*, Kluwer Academic Publishers, Netherlands, 1993.
14. W. J. Swiatecki, *The rotating, charged or gravitating liquid drop and problems in nuclear physics and astronomy*, Proceedings of the International Colloquium on Drops and Bubbles, (eds. D. J. Collins, M. S. Plesset, and M. M. Saffren), Jet Propulsion Laboratory, Pasadena, California (1974), 52–78.

15. R. Tagg, L. Cammack, A. Croonquist, and T. C. Wang, *Rotating Liquid Drops: Plateau's Experiment Revisited*, National Aeronautics and Space Administration, JPL Publication 80-66, Jet Propulsion Laboratory, California Institute of Technology, Pasadena, CA, 1980.
16. T. G. Wang, E. H. Trinh, A. P. Croonquist, and D. D. Elleman, *Shapes of rotating free drops: Spacelab experimental results*, Phys. Rev. Lett. **56** (1986), 452–455.
17. H. C. Wente, *The symmetry of rotating fluid bodies*, Manuscripta Math. **39** (1982), 287–296.

DEPARTMENT OF MATHEMATICS, UNIVERSITY OF CALIFORNIA AT SAN DIEGO, LA JOLLA, CALIFORNIA 92093, U.S.A.

DEPARTMENT OF MATHEMATICAL SCIENCES, SAN DIEGO STATE UNIVERSITY, SAN DIEGO, CALIFORNIA 92182, U.S.A.